Nanoscale

Cite this: *Nanoscale*, 2012, **4**, 152

www.rsc.org/nanoscale

PAPER

Very large magnetoresistive graphene disk with negative permittivity†

Jiahua Zhu,[a] Suying Wei,*[b] Neel Haldolaarachchige,[c] Jun He,[d] David P. Young[c] and Zhanhu Guo*[a]

Received 14th August 2011, Accepted 10th October 2011
DOI: 10.1039/c1nr11101a

At room temperature a large magnetoresistance (MR) of up to 70% is observed in graphene. Both graphene size and surface functionality influence the MR behavior significantly. The conductivity increases linearly with increasing temperature and a unique negative permittivity over a wide frequency range from 10^3 to 10^6 Hz is observed at room temperature.

Introduction

Two dimensional (2D) single carbon atom thick graphene arranged as a honeycomb lattice has unique electron and phonon transport[1–5] and possesses wide potential applications such as nanoscale devices.[6–10] Both theoretical and experimental research efforts have indicated that the electronic energy dispersion in graphene is different from conventional 2D materials. Specifically, the electron and hole bands are linear near K and K' points of the Brillouin zone in 2D graphene. However, the electron energy depends quadratically on the electron momentum in a conventional 2D system.[11] Various unusual transport phenomena are related to the fact that graphene behaves as a 2D electronic system, and the conduction and valence bands meet at the Dirac point, where the Fermi energy position is located.[12]

Giant magnetoresistance (GMR), first discovered in alternating ferromagnetic iron and non-ferromagnetic chromium layers,[13] is defined as a large change in resistance when the relative orientation of the magnetic domains in adjacent layers is adjusted from anti-parallel to parallel under an applied magnetic field. Generally, a small quadratic MR is observed in a normal conductor and saturates at relatively low fields. However, a large unsaturated linear magnetoresistance (LMR) has been observed in several systems after introducing inhomogeneities into the host matrix. Single phased Sb along InSb grain boundaries,[14] MnAs nanoparticles in GaAs films[15] and slightly phosphorus-doped n-type silicon are a few examples.[16] To obtain the LMR, some specific characteristics should preexist in these materials, including an approximately linear energy spectrum, carriers of low effective mass, and a zero band gap. The unique band structure of graphene makes it one of the best candidates for studying LMR. To the best of our knowledge, most of the current research on the MR behavior of graphene is still in a state of modeling and theoretical prediction.[17–20] Muñoz-Rojas *et al.* predict a 100% MR in a device made entirely out of carbon by computing the spin-polarized electron transport across a finite zigzag graphene ribbon bridged by two metallic graphene electrodes.[18] Very few experimental results have been reported until recently. Bai *et al.*[21] and Friedman *et al.*[22] have found MR behavior in graphene nanoribbons (50% MR at room temperature) and multilayer epitaxial graphene (~80% MR at room temperature), respectively. However, these experimental results are observed in highly complex nanoelectronic devices. What will the results be if the device size is scaled up from nanoscale to micro-, or even to macro-scale? For a bulk graphene sample, the question regarding how the individual graphene nanoparticle size and its surface functionality affect the bulk MR property still remains.

Related to its unusual electronic band structure, graphene has triggered great interests in plasmonics with a great promise to achieve not only nanophotonics with light scales substantially smaller than its wavelength[23,24] but also negative refraction index,[25] characteristic of metamaterials, which have potential wide applications including super lensing[26] and cloaking.[27] For example, Jablan *et al.* investigated plasmons in doped graphene at infrared frequencies.[12] Hill *et al.* studied the collective plasmon excitations as a function of frequency.[28] Tudorovskiy and Mikhailov found a low-frequency 2D plasmon near the corners of the hexagonal-shaped Brillouin zone.[29] Non-linear surface waves near the Dirac point were also investigated by Shen *et al.*[30] Despite the aforementioned theoretical predictions in the emerging plasmonics area, experimental investigations are critically lacking. However, the frequency dependent negative permittivity of the 2D graphene together with large MR is rarely reported. In this paper, the magnetotransport properties were investigated for compressed disk-shaped graphenes with a diameter of 20 mm and a thickness of ~0.5 mm.

[a]*Integrated Composites Laboratory (ICL), Dan F. Smith Department of Chemical Engineering, Lamar University, Beaumont, Texas, 77710, USA. E-mail: zhanhu.guo@lamar.edu; Tel: +1(409) 880-7654*
[b]*Department of Chemistry and Biochemistry, Lamar University, Beaumont, Texas, 77710, USA. E-mail: suying.wei@lamar.edu; Tel: +1 (409) 880-7976*
[c]*Department of Physics and Astronomy, Louisiana State University, Baton Rouge, Louisiana, 70803, USA*
[d]*National Center for Nanoscience and Technology, Beijing, 100190, China*
† Electronic supplementary information (ESI) available: SEM of the as-received graphene samples and the schematic mechanism of electron transportation, Fig. S1 and S2. See DOI: 10.1039/c1nr11101a

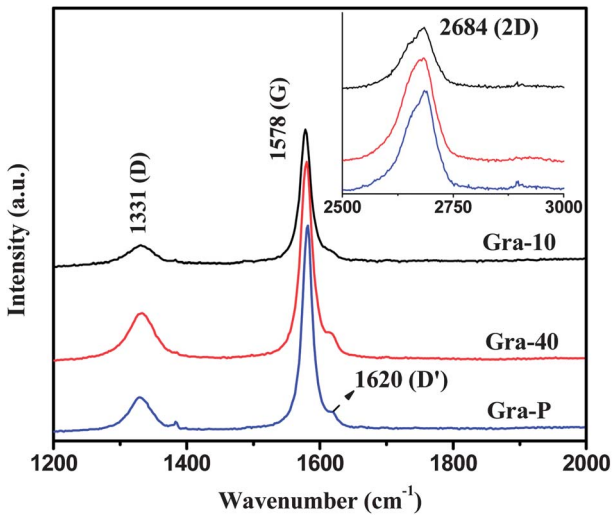

Fig. 1 Raman spectra of the graphene samples: Gra-10, Gra-40 and Gra-P. The inset shows the sharp 2D peak of each sample.

Experimental

The sample morphology was characterized by scanning electron microscopy (SEM, refer to Fig. S1 in the ESI†). Three different-sized graphenes (N008-100-P-10, *XY*: 5–10 μm, *Z*: 50–100 nm; N008-100-P-40, *XY*: ≤44 μm, *Z*: 50–100 nm; N006-010-P, *XY*: ≤14 μm, *Z*: <40 nm, Angstron Materials Inc., USA. For brevity, Gra-10, Gra-40 and Gra-P are used to represent the three different graphenes) were studied. No surfactant was used in Gra-10 and Gra-40, while sodium dodecylbenzenesulfonate (SDBS) was introduced into Gra-P. The temperature-dependent conductivity, MR and room temperature dielectric properties were investigated. The effects of graphene size and surface functionality on the properties were studied and are detailed here.

Results and discussion

Fig. 1 compares the Raman spectra of the three different graphene samples. There are three intense features in the Raman spectra of graphene. The two most important of these are the D band at 1331 cm^{-1} and the G band at 1578 cm^{-1}. The edge-induced disordered D band[31] is related to the presence of sp^3 defects, while the G band is related to the in-plane vibration of sp^2 carbon atoms, which is a doubly degenerate (transverse-optical and longitudinal-optical) phonon mode (E_{2g} symmetry) at the Brillouin zone center. The D band is a marker of defect density, and its relatively low intensity as compared to that of the G band indicates a small proportion of defects in these samples. The D′ band at 1620 cm^{-1} [32,33] can partially merge with the G band due to a nonzero phonon density of states above the G band. Such phonons, which are usually Raman-inactive, become active with a weak peak, Fig. 1, due to the defect-induced phonon confinement.[33] The observed 2D (or G′) band at 2684 cm^{-1} is due to the two phonons with opposite momentum in the highest optical branch near the *K* point of the Brillouin zone.[34,35] The presence of a sharp and symmetric 2D band is used as a fingerprint to differentiate single or bilayer graphene from multilayer graphene.[36] In this work, the broad and nonsymmetrical 2D band (inset of Fig. 1) indicates a multilayer structure, *i.e.* more than five layers.[37]

Fig. 2 shows the MR at 130 and 290 K for three graphene samples with different sizes. MR is calculated using eqn (1):

$$\mathrm{MR}(\%) = \frac{R(H) - R(0)}{R(0)} \times 100 \qquad (1)$$

where $R(0)$ and $R(H)$ are the resistance at zero field and at any applied field H, respectively. The peak MR is observed to vary from 42 to 64% at 130 K and 9 T (Fig. 2a), while the MR shows a relatively higher value in the range of 56–72% at 290 K and 9 T (Fig. 2b). The MR at both temperatures shows no sign of saturation, even at 9 T.

The slope of the MR curves changes near the crossover field, H_c (the field at which the data become linear). For all the samples measured, H_c is roughly 1 T. The slope change across H_c is attributed to the switching from quantum to classical LMR behavior.[14] It is interesting to observe that the MR not only persists, but even increases at room temperature (Fig. 2b). Such behavior was also observed in multilayer epitaxial graphene[22] with similar MR values. A recent study on graphene nano-ribbons showed a negative MR of nearly 100% at low temperatures and over 50% MR at room temperature.[38] The

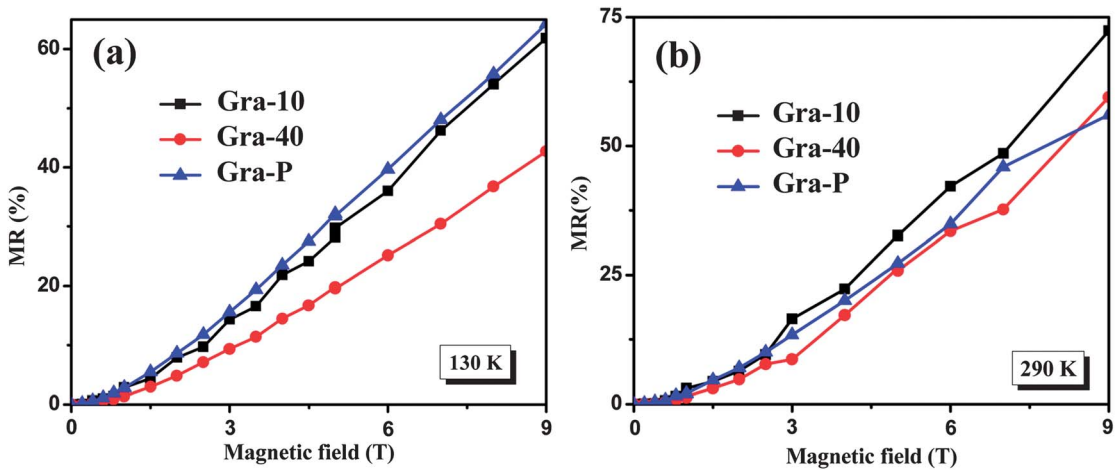

Fig. 2 The MR of Gra-10, Gra-40 and Gra-P at (a) 130 K and (b) 290 K.

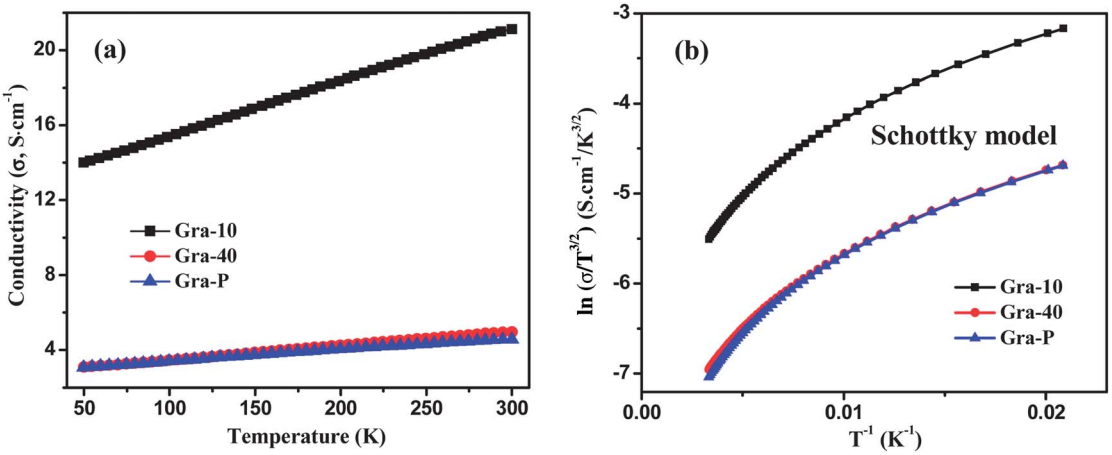

Fig. 3 (a) Temperature dependent conductivity of Gra-10, Gra-40 and Gra-P. (b) Schottky barrier-limited charge transport model.

observed MR phenomenon was attributed to the reduction of quantum confinement through the formation of cyclotron orbits and the delocalization effect under a perpendicular field.[39–41]

Compared to the theoretical studies on ultra-small graphene devices with a predicted 100% MR at 10 T,[18] a linear extrapolation of the room temperature MR of Gra-10 at 10 T gives a value of ~90%, close to the theoretical prediction. The compressed graphene disks with a diameter of 20 mm and a thickness of ~0.5 mm show size-dependent MR behaviors, Fig. 2a and b. Gra-10 shows a better MR performance than Gra-40 at both 130 and 290 K. Gra-10 consists of a larger number of stacked graphene sheets, thereby being more significantly affected by a perpendicular field. However, Gra-P, with the smallest sheet size, shows the highest MR at 130 K among all the three samples. At 130 K, the MR strictly follows a size-dependent behavior, *i.e.*, the MR increases as the graphene sheet decreases. This is likely due to the larger disorder inherent with the Gra-P sample, and thus less quantum confinement through the formation of cyclotron orbits and the delocalization effect under a perpendicular field.[40,42] The lower MR in the Gra-P sample at 290 K is attributed to the activated alkyl chain segmentation of surfactant SDBS on the graphene surface, which disturbs the charge delocalization.

Fig. 3a shows the conductivity (σ) as a function of temperature for the three different graphene samples. Gra-10 exhibits the highest σ over the whole temperature range, which starts from 14 S cm^{-1} at ~50 K to 21.1 S cm^{-1} at 300 K. The σ curves of Gra-40 and Gra-P are very similar to each other, which are about 25% lower than that of Gra-10 at 50 K. The lower σ of the Gra-40 sample is due to the larger fraction of parallel-oriented graphene sheets (refer to Fig. S2 in the ESI†). Graphite with a large *c*-axis resistivity[43] has less effective electron transport in the vertical direction. As for the Gra-P sample, even though the particle dimension is lower than that of Gra-10, more sheets are expected to be oriented along the *c*-axis. The much lower σ is due to the existence of surfactant on the sheet surface, which prevents efficient electron transport between graphene sheets. With increasing temperature, the curves of both Gra-40 and Gra-P start at 3.1 S cm^{-1} at 50 K and increase to 5 and 4.5 S cm^{-1}, respectively (Fig. 3a).

For all the three samples, $d\sigma/dT > 0$ indicates semiconductor behavior from 50 to 300 K.[44] However, the observed linear pattern rather than the thermally activated Arrhenius law, Fig. 3a, suggests the absence of a band gap. To determine that the resistance comes from either the intrinsic sheet resistance or the contact resistance between electrodes and the sample surface, the resistivity data are fitted with a Schottky barrier-limited charge transport model, eqn (2):[45,46]

$$I(T) \propto T^{3/2} \exp(-1/T) \quad (2)$$

where I represents the source-drain current (replaced by σ in this work since σ and I are linearly dependent) and T is the absolute temperature. An exponential rather than a linear fitting curve from the Schottky transport model, Fig. 3b, strongly indicates that the measured resistivity is mainly governed by the intrinsic sheet resistance rather than the contact resistance.[47]

The real permittivity (ε') of the three graphene samples is studied within the frequency range of 20 Hz to 2 MHz. All three samples show a similar dielectric curve, where ε' starts at an extremely high positive value at low frequency, decreases sharply with increasing frequency, crosses zero, and remains negative at high frequency. It is interesting to observe that Gra-10 shows the largest positive ε' of about 4.7×10^5 at 20 Hz, which is almost twice the value observed in Gra-40 and Gra-P at the same frequency. At the same time, the largest negative permittivity is also observed in Gra-10, as ε' varies within the range of −4000 to −2000 (Fig. 4a), while ε' for Gra-10 and Gra-P falls in the range of −500 to −200 (Fig. 4b and c). The switching frequency, where ε' crosses zero for each sample, is 1310, 1876 and 2060 Hz (marked in Fig. 4a–c), respectively.

The negative ε' at higher frequency in 2D graphene arises from the unique electronic energy dispersion, *i.e.* surface plasmons. The unusual electron transport phenomena arise from the freely tunable Fermi energy in graphene, which can be affected by an external electromagnetic field.[28] Classical 2D plasmon behavior is given by $w_0 \propto n^{1/2}$, where w_0 (plasmon frequency) is defined as $w_0 = (g_s g_v e^2 E_F/2k)^{1/2}$, n is the carrier (electron and hole) density, g_s and g_v are the spin and valley degeneracies, E_F is the Fermi energy, and k is the background lattice dielectric constant of the system.[11] In graphene, however, the density dependent plasmon

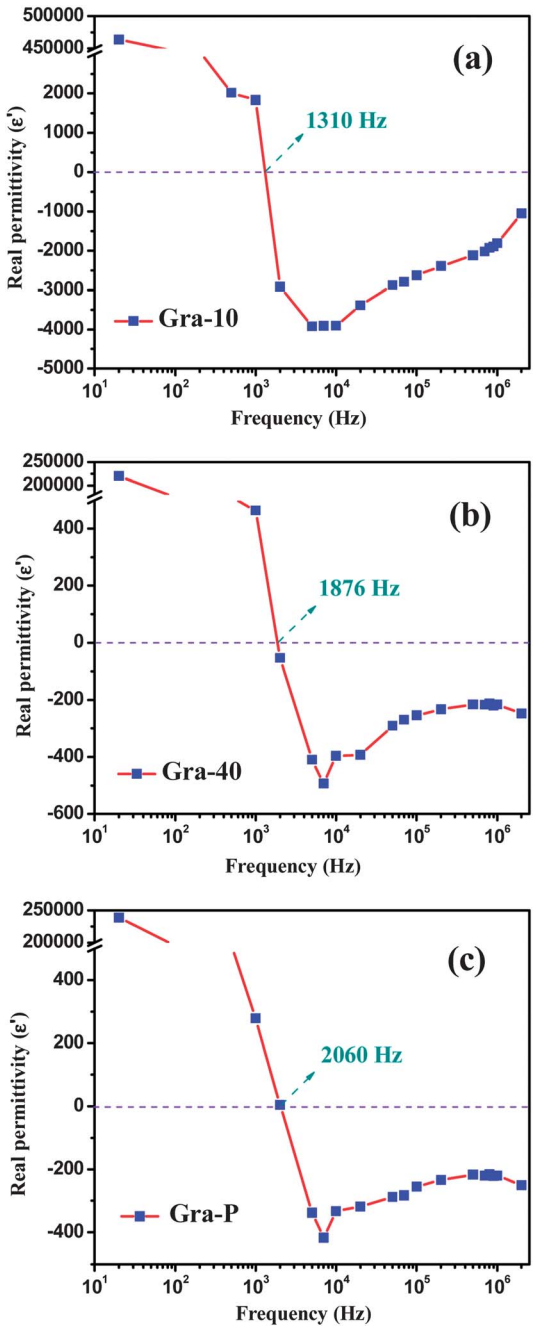

Fig. 4 Frequency dependent permittivity of (a) Gra-10, (b) Gra-40 and (c) Gra-P.

frequency shows a $w_0 \propto n^{1/4}$ behavior. This unique behavior would lead to a decrease in the plasmon frequency as predicted by the random-phase approximation, which is in good agreement with the negative permittivity observed at low frequencies. More interestingly, the increase in the switching frequency from Gra-10, Gra-40 to Gra-P corresponds well with the increase in their resistivity, indicating a higher charge carrier density within Gra-10, thereby facilitating the electron transport as well as plasmon resonance in the system. Considering the interlayer hopping in these multilayer graphenes, the in-phase plasmon mode is qualitatively unaffected by tunneling. However, the out-of-phase plasmon mode develops a long wavelength gap in the presence of tunneling,[48,49] which explains well the sharp decrease of ε'. These special characteristics make graphene suitable for wide technological applications involving plasmons, such as coherent terahertz sources based on plasmon amplification[50] and optoelectronics due to the existence of the transverse electromagnetic mode in graphene.[51]

Conclusions

In conclusion, a large MR of 40–60% at 130 K in all the three different bulk graphene disks and an increased MR of 50–70% at 290 K for the Gra-10 and Gra-40 samples are observed, while SDBS on the Gra-P surface results in a lower MR at 290 K than that at 130 K. A linear increase of conductivity with increasing temperature indicates a semiconductor-like behavior without a bandgap. The experimentally observed negative permittivity over a wide frequency range reveals the synergistic effects of in-plane and out-of-plane surface plasmon resonance. These unique electronic properties may lead to new classes of advanced materials to be widely applied as magnetic sensors,[14] ultra-high density memory storage,[52] super lenses and wave-guided optics.[53]

Acknowledgements

This project is supported by the Research Start-up Grant and the support from National Science Foundation-Nanoscale Interdisciplinary Research Team and Materials Processing and Manufacturing (CMMI 10-30755) for TGA and DSC is appreciated. D. P. Young acknowledges support from the NSF under grant no. DMR 10-05764. The authors appreciate Angstron Materials, Inc. for supplying graphene materials.

References

1 K. S. Novoselov, D. Jiang, F. Schedin, T. J. Booth, V. V. Khotkevich, S. V. Morozov and A. K. Geim, *Proc. Natl. Acad. Sci. U. S. A.*, 2005, **102**, 10451.
2 Y. Zhang, Y.-W. Tan, H. L. Stormer and P. Kim, *Nature*, 2005, **438**, 201.
3 K. S. Novoselov, A. K. Geim, S. V. Morozov, D. Jiang, Y. Zhang, S. V. Dubonos, I. V. Grigorieva and A. A. Firsov, *Science*, 2004, **306**, 666.
4 D. A. Abanin, S. V. Morozov, L. A. Ponomarenko, R. V. Gorbachev, A. S. Mayorov, M. I. Katsnelson, K. Watanabe, T. Taniguchi, K. S. Novoselov, L. S. Levitov and A. K. Geim, *Science*, 2011, **332**, 328.
5 J. H. Seol, I. Jo, A. L. Moore, L. Lindsay, Z. H. Aitken, M. T. Pettes, X. Li, Z. Yao, R. Huang, D. Broido, N. Mingo, R. S. Ruoff and L. Shi, *Science*, 2010, **328**, 213.
6 A. Dimiev, D. V. Kosynkin, A. Sinitskii, A. Slesarev, Z. Sun and J. M. Tour, *Science*, 2011, **331**, 1168.
7 P. Avouris, *Nano Lett.*, 2010, **10**, 4285.
8 V. M. Karpan, G. Giovannetti, P. A. Khomyakov, M. Talanana, A. A. Starikov, M. Zwierzycki, J. van den Brink, G. Brocks and P. J. Kelly, *Phys. Rev. Lett.*, 2007, **99**, 176602.
9 Z. Wei, D. Wang, S. Kim, S.-Y. Kim, Y. Hu, M. K. Yakes, A. R. Laracuente, Z. Dai, S. R. Marder, C. Berger, W. P. King, W. A. de Heer, P. E. Sheehan and E. Riedo, *Science*, 2010, **328**, 1373.
10 X. Li, W. Cai, J. An, S. Kim, J. Nah, D. Yang, R. Piner, A. Velamakanni, I. Jung, E. Tutuc, S. K. Banerjee, L. Colombo and R. S. Ruoff, *Science*, 2009, **324**, 1312.
11 E. H. Hwang and S. Das Sarma, *Phys. Rev. B: Condens. Matter Mater. Phys.*, 2007, **75**, 205418.
12 M. Jablan, H. Buljan and M. Soljaccaronicacute, *Phys. Rev. B: Condens. Matter Mater. Phys.*, 2009, **80**, 245435.

13 M. N. Baibich, J. M. Broto, A. Fert, F. N. Van Dau, F. Petroff, P. Etienne, G. Creuzet, A. Friederich and J. Chazelas, *Phys. Rev. Lett.*, 1988, **61**, 2472.
14 J. Hu and T. F. Rosenbaum, *Nat. Mater.*, 2008, **7**, 697.
15 H. G. Johnson, S. P. Bennett, R. Barua, L. H. Lewis and D. Heiman, *Phys. Rev. B: Condens. Matter Mater. Phys.*, 2010, **82**, 085202.
16 M. P. Delmo, S. Yamamoto, S. Kasai, T. Ono and K. Kobayashi, *Nature*, 2009, **457**, 1112.
17 W. Y. Kim and K. S. Kim, *Nat. Nanotechnol.*, 2008, **3**, 408.
18 F. Muñoz-Rojas, J. Fernández-Rossier and J. J. Palacios, *Phys. Rev. Lett.*, 2009, **102**, 136810.
19 L. Brey and H. A. Fertig, *Phys. Rev. B: Condens. Matter Mater. Phys.*, 2007, **76**, 205435.
20 S. Bala Kumar, M. B. A. Jalil, S. G. Tan and G. Liang, *J. Appl. Phys.*, 2010, **108**, 033709.
21 J. Bai, R. Cheng, F. Xiu, L. Liao, M. Wang, A. Shailos, K. L. Wang, Y. Huang and X. Duan, *Nat. Nanotechnol.*, 2010, **5**, 655.
22 A. L. Friedman, J. L. Tedesco, P. M. Campbell, J. C. Culbertson, E. Aifer, F. K. Perkins, R. L. Myers-Ward, J. K. Hite, C. R. Eddy, G. G. Jernigan and D. K. Gaskill, *Nano Lett.*, 2010, **10**, 3962.
23 W. L. Barnes, A. Dereux and T. W. Ebbesen, *Nature*, 2003, **424**, 824.
24 A. Karalis, E. Lidorikis, M. Ibanescu, J. D. Joannopoulos and M. Soljačić, *Phys. Rev. Lett.*, 2005, **95**, 063901.
25 V. M. Shalaev, *Nat. Photonics*, 2007, **1**, 41.
26 J. B. Pendry, *Phys. Rev. Lett.*, 2000, **85**, 3966.
27 W. Cai, U. K. Chettiar, A. V. Kildishev and V. M. Shalaev, *Nat. Photonics*, 2007, **1**, 224.
28 A. Hill, S. A. Mikhailov and K. Ziegler, *EPL*, 2009, **87**, 27005.
29 T. Tudorovskiy and S. A. Mikhailov, *Phys. Rev. B: Condens. Matter Mater. Phys.*, 2010, **82**, 073411.
30 M. Shen, L.-X. Ruan, X. Chen, J.-L. Shi, H.-X. Ding, N. Xi and Q. Wang, *J. Opt. (Bristol, U. K.)*, 2010, **12**, 085201.
31 X. Li, G. Zhang, X. Bai, X. Sun, X. Wang, E. Wang and H. Dai, *Nat. Nanotechnol.*, 2008, **3**, 538.
32 M. J. O'Connell, P. Boul, L. M. Ericson, C. Huffman, Y. Wang, E. Haroz, C. Kuper, J. Tour, K. D. Ausman and R. E. Smalley, *Chem. Phys. Lett.*, 2001, **342**, 265.
33 S. D. Bergin, V. Nicolosi, H. Cathcart, M. Lotya, D. Rickard, Z. Sun, W. J. Blau and J. N. Coleman, *J. Phys. Chem. C*, 2008, **112**, 972.
34 M. Lotya, Y. Hernandez, P. J. King, R. J. Smith, V. Nicolosi, L. S. Karlsson, F. M. Blighe, S. De, Z. Wang, I. T. McGovern, G. S. Duesberg and J. N. Coleman, *J. Am. Chem. Soc.*, 2009, **131**, 3611.
35 A. C. Ferrari, *Solid State Commun.*, 2007, **143**, 47.
36 J. Lu, J.-X. Yang, J. Wang, A. Lim, S. Wang and K. P. Loh, *ACS Nano*, 2009, **3**, 2367.
37 A. C. Ferrari, J. C. Meyer, V. Scardaci, C. Casiraghi, M. Lazzeri, S. Piscanec, D. Jiang, K. S. Novoselov, S. Roth and A. K. Geim, *Phys. Rev. Lett.*, 2006, **97**, 187401.
38 J. Bai, R. Cheng, F. Xiu, L. Liao, M. Wang, A. Shailos, K. L. Wang, Y. Huang and X. Duan, *Nat. Nanotechnol.*, 2010, **5**, 655.
39 N. M. R. Peres, A. H. Castro Neto and F. Guinea, *Phys. Rev. B: Condens. Matter Mater. Phys.*, 2006, **73**, 241403.
40 N. M. R. Peres, A. H. Castro Neto and F. Guinea, *Phys. Rev. B: Condens. Matter Mater. Phys.*, 2006, **73**, 195411.
41 J. Liu, A. R. Wright, C. Zhang and Z. Ma, *Appl. Phys. Lett.*, 2008, **93**, 041106.
42 C. Ritter, S. S. Makler and A. Latgé, *Phys. Rev. B: Condens. Matter Mater. Phys.*, 2008, **77**, 195443.
43 K. Matsubara, K. Sugihara and T. Tsuzuku, *Phys. Rev. B: Condens. Matter Mater. Phys.*, 1990, **41**, 969.
44 S. Chakrabarti, D. Banerjee and R. Bhattacharyya, *J. Phys. Chem. B*, 2002, **106**, 3061.
45 X. Wu, M. Sprinkle, X. Li, F. Ming, C. Berger and W. A. de Heer, *Phys. Rev. Lett.*, 2008, **101**, 026801.
46 A. Anwar, B. Nabet, J. Culp and F. Castro, *J. Appl. Phys.*, 1999, **85**, 2663.
47 A. B. Kaiser, C. Gómez-Navarro, R. S. Sundaram, M. Burghard and K. Kern, *Nano Lett.*, 2009, **9**, 1787.
48 S. Das Sarma and E. H. Hwang, *Phys. Rev. Lett.*, 1999, **83**, 164.
49 S. Das Sarma and E. H. Hwang, *Phys. Rev. B: Condens. Matter Mater. Phys.*, 2004, **69**, 195305.
50 V. Ryzhii, M. Ryzhii and T. Otsuji, *J. Appl. Phys.*, 2007, **101**, 083114.
51 S. A. Mikhailov and K. Ziegler, *Phys. Rev. Lett.*, 2007, **99**, 016803.
52 E. U. Stützel, M. Burghard, F. Traversi, F. Nichele and R. Sordan, *Small*, 2010, **6**, 2821.
53 F. Wang, Y. Zhang, C. Tian, C. Girit, A. Zettl, M. Crommie and Y. R. Shen, *Science*, 2008, **320**, 206.

